NUMERICAL SOLUTION OF AMERICAN OPTION PRICING PROBLEMS UNDER STOCHASTIC VOLATILITY

Ferran Fuster Valls

Trabajo de investigación 019/009

Máster en Banca y Finanzas Cuantitativas

Director/a: Dr. Rafael Company Rossi
Dr. Lucas Jódar Sánchez

Universidad Complutense de Madrid

Universidad del País Vasco

Universidad de Valencia

Universidad de Castilla-La Mancha

www.finanzascuantitativas.com

Numerical solution of American option pricing problems under stochastic volatility

MSc thesis

Ferran Fuster Valls

Máster en Banca y Finanzas Cuantitativas

Directors: Rafael Company Rossi and Lucas Jódar Sánchez

Universidad Complutense de Madrid
Universidad del País Vasco
Universitat de València
Universidad de Castilla-La Mancha

Abstract

This work provides numerical solutions for American options under the mean-reversion stochastic volatility Heston model. Firstly, the spatial cross-derivative of the partial differential equation (PDE) is removed by the classical technique for reduction of second-order linear PDE to canonical form, achieving a diffusion-advection-reaction (DAR) problem. Later, the DAR problem solution is constructed starting with a semi-discretization approach followed by a full discretization using an exponential time differencing (ETD) scheme. Since a good model can be wasted with a careless numerical method, numerical analysis is studied including the positivity and stability of the solution. Finally numerical experiments were computed to prove its competitiveness with other relevant methods in the literature.

Contents

1 Introduction **1**

1.1 American options . . . 1

1.2 Stochastic volatility . . . 6

1.3 Option pricing under stochastic volatility . . . 9

2 Transformation of the problem **10**

2.1 Motivation . . . 10

2.2 The new variables . . . 11

2.3 Artificial Boundary conditions . . . 13

2.4 Domain assumptions . . . 14

3 Semi-discretization and ETD scheme **15**

3.1 Discretization . . . 15

3.2 New variable . . . 16

3.3 Derivatives . . . 17

3.4 System of ODEs . . . 18

3.5 ETD method . . . 19

4 Positivity and stability **20**

4.1 Positivity . . . 21

4.2 Some definitions and properties . . . 21

4.3 Stability . . . 22

4.4 Induction principle . . . 24

5 Numerical experiments **25**

5.1 Results comparison . . . 26

5.2 Greeks . . . 28

5.3 Numerical convergence . . . 29

6 Conclusions **30**

Bibliography **32**

1 Introduction

The classic Black-Scholes model makes assumptions that are not empirically valid. The model is widely employed as a useful approximation to reality, but proper application requires understanding its limitations and constant volatility of the stock returns is one of them. In fact, this assumption is one of the biggest source of weakness, because the variance has been observed to be non-constant leading to models, such as GARCH, to model volatility changes. There are other approaches to model the asset volatility, as consider that follows a random process or, in other words, consider the volatility as a stochastic process. This point of view lead us to a Partial Differential Equation (PDE) different from the classic Black-Scholes, now there are involved two different variables, apart of the time: asset level S and variance ν. Deal with this PDE and the presence of cross-derivatives is a challenging task. It is even more difficult to deal with American options which allows to exercise the option at any time before the expiration date. But the solution to this problem is of great interest to the financial markets.

The main objective of this work is to present a numerical method, based on finite differences, to obtain solutions for the valuation of American put options under stochastic volatility. The tools that we have used to solve the problem are:

- Penalty term to deal with American options.
- Transformation of the problem to remove the cross-derivatives.
- Use of the method of lines, also called semi-discretization, that lead us to a system of Ordinary Differential Equations (ODE).
- Exponential Time Differencing method (ETD) to provide solution to the ODEs system.

Also numerical analysis of the proposed method is studied to guaranteed the goodness of the numerical solutions. This work is organized as follows. In the remainder of the Introduction section we present properly the details of dealing with American options and stochastic volatility. Section 2 addresses the problem transformation, which has the aim of remove cross derivatives and explain the new rhomboid numerical domain. The semi-discretization and the proposed ETD scheme are included in Section 3. In Section 4 the positivity, stability and boundedness of the numerical solution will be studied. Section 5 compare numerical results with other authors and compute the numerical order of convergence.

1.1 American options

Options contract gives its holder the right, but not the obligation, to buy or sell an underlying asset at a specified strike price during a certain period of time or on a specific date. Options have a limited life time, the maturity date fixes the time horizon. At this date the rights of the holder expire, and for later times the option is worthless. We talk about American options when the holder can exercise the option on any trading day on or before the maturity and, about European options, when the option can only be exercised at the maturity. For the valuation of European option on a non-dividend paying asset we have the classic model Black and Scholes (1973). This model led to a boom in options trading and provided mathematical legitimacy to the activities of the Chicago Board Options Exchange and other options markets around the world.

So, given that American options can be exercised at any time to maturity, they provide its holder greater rights than the European options, where early exercise is not allowed. Therefore American options prices have potentially higher value than the European. The following arbitrage argument shows how this can happen.

We consider a put option on a non-dividend paying asset. For every time before the maturity, there is a large range of asset value S for which the value of European put option is less than its intrinsic value (the payoff function). For example, the European put price for $S = 0$ is $P(0, t) = Ee^{-r(T-t)}$ that is below the payoff function evaluated at $S = 0$ whose value is the strike price E. We can see that at Figure 1. Suppose that S lies in this range, so that $P(S, t) < max(E - S, 0)$, and consider the effect of exercising the option. There is an obvious arbitrage opportunity: we can buy the asset S and the option for P and, if we immediately exercise the option, we thereby make a risk-free profit of $E - S - P$. Of course, such an opportunity would not last long before the value of the option was pushed up by the demand of arbitragers. We conclude that when the early exercise is permitted we must impose the constraint:

$$P(S, t) \geq max(E - S,\ 0). \tag{1}$$

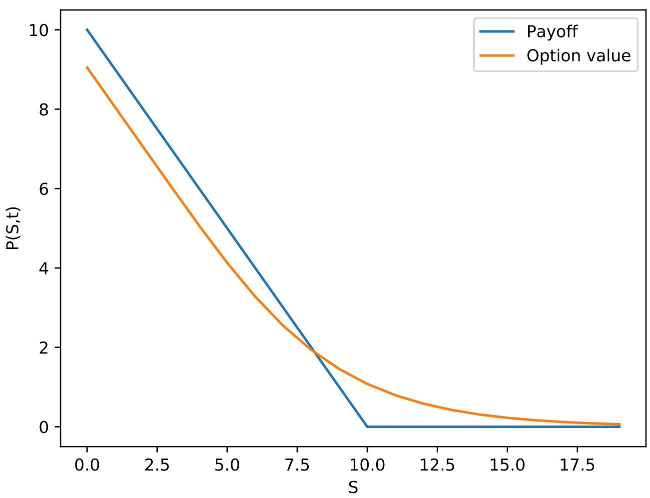

Figure 1: European put option with r = 0.1, σ = 0.4, t = T-1, E = 10 and the payoff function

We can also see that American options have different value than the European if we consider a call option on a dividend-paying asset. For a large values of S, the dominant behavior of the European option is

$$C(S, t) \sim Se^{-D_0(T-t)}.$$

This is because in the limit $S \to \infty$ the European call option becomes equivalent to the asset but without its dividend income. As we can see, for large S, European call lies below the payoff function $max(S - E, 0)$. See Figure 2. If the early exercise is allowed there is an arbitrage opportunity: buying the option, exercising it and selling the asset we obtain another risk-free profit of $S - E - C$. Therefore the American version of this call option must also be more valuable than the European, so it must satisfy the constraint:

$$C(S, t) \geq max(S - E,\ 0). \tag{2}$$

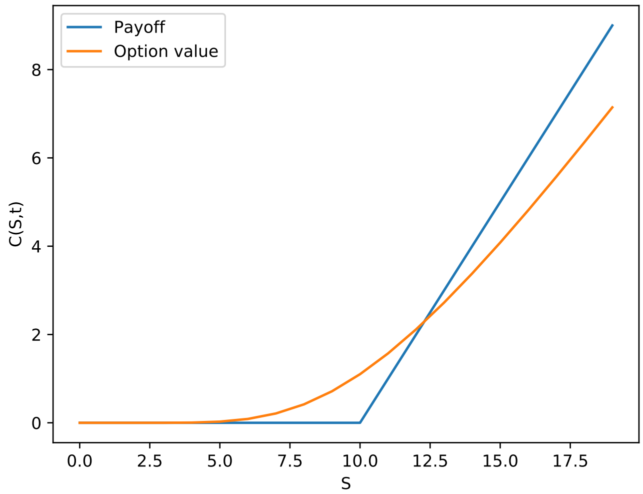

Figure 2: European call option with r = 0.1, σ = 0.4, t = T-1, E = 10, q = 0.17 and the payoff function

In both of these cases, there must be some values of S for which it is optimal, from the holder's point of view, to exercise the American option. The valuation of American options is therefore more complicated, since at each time we have to determine the option value and, for each value of S, whether or not the option should be exercised. This is what is known as a Free Boundary Problem (FBP). Typically, there exists at each time t a value of S which marks the boundary between two regions: to one side one should hold the option (continuation region) and to the other side one should exercise it (early exercise region). We denote this value, which in general varies with time, by $S^*(t)$, and refer to it as the optimal exercise price. McKean (1965) and van Moerbeke (1976) showed that this price varies with time until expiration. When we are dealing with European options we know which boundary conditions to apply and where to apply them, but with American options we do not know where to apply them. The unknown boundary $S^*(t)$ is for this reason called free boundary. This situation is common to many financial and physical problems.

An American option pricing problem can be specified by a set of four constraints:

1. Option value must be greater than or equal to the payoff function.
2. Black-Scholes equation is replaced by an inequality.
3. Option value must be a continuous function of S.
4. Option delta (its slope) must be continuous.

The first of this constraints has already been commented and it was due to the condition of absence of arbitrage opportunities. So that, if the option value is the same as the payoff function, the option should be exercised. But if it exceeds the payoff, the option satisfies the Black-Scholes equation. It turns out that these two statements can be combined into one inequality for the Black-Scholes equation, which is the second constraint.

Before going ahead, taking the time to maturity date $\tau = T - t$ as time variable, we define the

Black-Scholes operator:

$$\mathcal{L}(U) \equiv \frac{\partial U}{\partial \tau} - \frac{1}{2}\sigma^2 S^2 \frac{\partial^2 U}{\partial S^2} - rS\frac{\partial U}{\partial S} + rU.$$

And our second constraint:

$$\mathcal{L}(P) \geq 0. \tag{3}$$

Is easy to verify it. Consider an American put option, when $P = E - S$, for $S \leq E$, substitution in (3) gives $\mathcal{L}(P) = rE > 0$.

The third constraint follows from simple arbitrage. If there were a discontinuity persisted for more than an infinitesimal time, a portfolio of options only would make a risk-free profit if the asset price ever reach the value at which discontinuity occurred.

We do not know the position of $S^*(t)$ but we must impose two conditions to: the option value at $S^*(t)$ and the position of $S^*(t)$. The continuity of the option value, also at the free boundary (third condition), provides us the first condition:

$$P(S^*, t) = max(E - S^*,\ 0), \quad C(S^*, t) = max(S^* - E,\ 0). \tag{4}$$

The fourth constraint, which imposes the continuity of option delta, even at $S^*(t)$, provides us the second condition. Using (1), (2) and arbitrage arguments it can be shown that the slope is -1 for puts and +1 for calls. More details at (P.Wilmott et al., 1995, section 7.4).

$$\frac{\partial P}{\partial S}(S^*, t) = -1, \quad \frac{\partial C}{\partial S}(S^*, t) = 1. \tag{5}$$

In summary, for an American put option, the valuation problem can be written as a free boundary problem as follows. For each time t, we must divide the S axis into two distinct regions. The first, $0 \leq S < S^*(t)$, is where early exercise is optimal and:

$$P = E - S, \quad \mathcal{L}(P) \geq 0.$$

In the other region, $S^*(t) < S < \infty$, early exercise is not optimal and:

$$P > E - S, \quad \mathcal{L}(P) = 0.$$

The boundary conditions at $S = S^*(t)$ are that P and its slope (delta) are continuous:

$$P(S^*, t) = max(E - S^*,\ 0), \quad \frac{\partial P}{\partial S}(S^*, t) = -1. \tag{6}$$

We can think of these as being one boundary condition to determine the option value on the free boundary, and the other to determine the location of the free boundary.

Usually explicit exact solutions of free boundary problems are not available.. The hard question is not only finding a solution but also find one that include the free boundary. Several references show us about two different methodologies to find this free boundary: one analytical and other numerical. About the first one, Geske and Johnson (1984) obtained closed-form solution for

American put options by a series of compound functions. The numerical approach, which is widely used, obtain the free boundary discretizing the continuous problem by finite differences. There is a lot of research about the different numerical schemes but one of the first was Brennan and Schwartz (1978). This scheme allows different types of finite differences: explicit, implicit, Runge-Kutta, etc. Other related researches are Hull and White (1990), Duffy (2006), Tangman et al. (2008), Zhu and Chen (2011) and Kim et al. (2013).

It is clear that free boundary calculus greatly increases the problems difficulty. So, it is worth the effort of attempting to reformulate the problem in such a way as to eliminate any explicit dependence on the free boundary. One way is consider a Linear Complementarity Problem (LCP) and look for an analogy to American pricing problem. For a put option value P, we have:

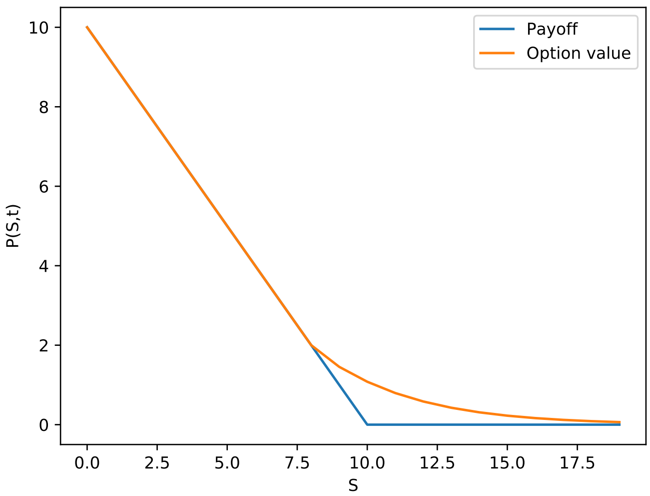

Figure 3: American put option problem

$$\text{If } P > max(E - S,\ 0), \quad \text{then BS equation } \mathcal{L}(P) = 0.$$

$$\text{If } P = max(E - S,\ 0), \quad \text{then BS equation } \mathcal{L}(P) > 0.$$

Therefore we can rewrite the American option pricing problem as a linear complementary problem:

$$\begin{cases} \mathcal{L}(P)(P - max(E - S,\ 0)) = 0 \\ \mathcal{L}(P) \geq 0 \\ P - max(E - S,\ 0) \geq 0 \end{cases} \tag{7}$$

With the following boundary conditions:

$$P(S,T) = max(E - S, 0)$$
$$P(0,t) = E \tag{8}$$
$$P(S,t) = 0, S \to \infty$$

Even though LCP is not the only way to avoid the calculus of $S^*(t)$. There are alternatives as, for example, the penalty methods. See Forsyth and Vetzal (2002) and Nielsen et al. (2002). Penalty method applied on American options is based on the simple idea of replacing the Black-Scholes inequation (3) by the following Partial Differential Equation (PDE):

$$\frac{\partial U}{\partial t} + \frac{1}{2}\sigma^2 U^2 \frac{\partial^2 U}{\partial S^2} + rS\frac{\partial U}{\partial S} - rU + f(U) = 0 \tag{9}$$

Where $f(U)$, called penalty term, is a non linear function of U. There are many options to choose a penalty term. One of them, for American put options, is take a similar form as in Forsyth and Vetzal (2002):

$$f(E,S,U) = \lambda\, max(E - S - U,\ 0) = \begin{cases} 0 & \text{if} \quad U > E - S \\ \lambda(E - S - U) & \text{if} \quad U \leq E - S \end{cases} \tag{10}$$

Where $\lambda \geq 0$ and, when $\lambda \to \infty$, the solution satisfy the constraint $U - (E - S) \geq 0$. Note that the penalty term is only active when the option value is less than the payoff and his objective is push the option value up to the payoff function. Other option is choosing a penalty form as in Nielsen et al. (2002):

$$f(U) = \frac{\epsilon C}{U + \epsilon - (E - S)}$$

Where $C \geq rE$ is a positive constant and $0 < \epsilon \ll 1$ is the regulation term.

It is important to note that the both approaches LCP and penalty method avoid the calculation of $S^*(t)$ and the complexity that this entails. In our work, we choose a penalty method with the form (10) to solve American option pricing problems.

1.2 Stochastic volatility

The classic Black-Scholes model makes the strong assumption of constant volatility of the stock returns. Several works show that volatility has a lot of properties and behaviors, but also that it is not exactly constant. The principal fact to prove it is the existence of the called "volatility smile" (Hull, 2018, chapter 20). This phenomenon arise when we try to fit de Black-Scholes equation to market option prices. The only unknown parameter in the model, given market data, is the volatility. So, if we extract from the model the called implied volatility from a group of options which only differs in the strike price, we will see that this volatilities are not constant. In fact, if we graph implied volatilities against strike prices for a given expiry yields to skewed "smile" instead of the expected flat surface.

A related concept is the so called term structure of volatility, which describes how (implied) volatility differs for related options with different maturities. An implied volatility surface is a 3-D plot that plots volatility smile and term structure of volatility in a consolidated three-dimensional surface for all options on a given underlying asset.

Modelling the volatility smile is an active area of research in quantitative finance, and better pricing models such as extensions of Black-Scholes model partially address this issue. Generally there are three main approaches.

Local volatility model treat volatility as a function of both the current asset level $S(t)$ and time t. The concept was developed in continuous-time by Dupire (1994) and in discrete-time by Derman and Kani (1994). Jump diffusion models, where the stock returns are a non-continuous function of time, allows big changes to asset prices. The first jump diffusion model was introduced by Merton (1976). Finally, the Stochastic Volatility (SV) models provides dynamics to volatility or variance by an Stochastic Differential Equation (SDE). One of the most widely used is Heston model (1993) which provides a closed-form solution for European options on a non-dividend paying asset.

SV models are useful because they explain in a self-consistent way why options with different strikes and expirations have different Black-Scholes implied volatilities. Moreover, unlike alternative models that can fit the smile, SV models assume realistic dynamics for the underlying asset.

Consider the daily log returns of an arbitrary asset. For large periods, the histogram of this log returns will be highly peaked and fat-tailed relative to the normal distribution. A Q-Q plot would show us just how extreme the tails of the empirical distribution of returns are relative to the normal distribution. Another feature that we could see is the so-called volatility clustering: "large changes tend to be followed by large changes, of either sign, and small changes tend to be followed by small changes" Mandelbrot (1967).

Fat tails and the high central peak are characteristics of mixtures of distributions with different variances. This motivates us to model variance as a random variable. The volatility clustering feature implies that volatility (or variance) is auto-correlated. In the model, this is a consequence of the mean reversion of volatility. Note that simple jump-diffusion models do not have this property: after a jump, the stock price volatility does not change.

There is a simple economic argument that justifies the mean reversion of volatility. If volatility were not mean reverting the probability of the volatility of any asset being between 1% and 100% would be rather low. Since we believe that it is overwhelmingly likely that the volatility in fact lie in that range, we deduce that volatility must be mean reverting.

In this work we choose a SV model with mean reversion, the famous Heston model, to price American put options. Heston model, with real-world dynamics is specified as follows:

$$\begin{aligned} dS(t) &= \mu S(t)dt + \sqrt{\nu(t)}S(t)dW_1, \\ d\nu(t) &= \kappa(\theta - \nu(t))dt + \sigma\sqrt{\nu(t)}dW_2, \\ dW_1 dW_2 &= \rho dt. \end{aligned} \tag{11}$$

With non-negative constants κ, θ, σ and instantaneous correlation $\rho \in (-1, 1)$. The variance process thus follows a square root process, also known as a CIR process from its use as a model for short-term interest rates by Cox et al. (1985) although the square root process goes back to Feller (1951). This kind of processes are bounded below by zero and, if the Feller condition is satisfied: $2\kappa\theta \geq \sigma^2$, the boundary cannot be achieved.

Applying Itô lemma and standard arbitrage arguments to (11) we acheieve a partial differential equation for the price $U = U(S, \nu, t)$ of a contingent claim:

$$\frac{\partial U}{\partial t} + \frac{1}{2}\nu S^2 \frac{\partial^2 U}{\partial S^2} + \rho\sigma\nu S \frac{\partial^2 U}{\partial S \partial \nu} + \frac{1}{2}\sigma^2 \nu \frac{\partial^2 U}{\partial \nu^2} + rS\frac{\partial U}{\partial S} + \Big(\kappa(\theta - \nu) - \phi\Big)\frac{\partial U}{\partial \nu} - rU = 0. \tag{12}$$

Where ϕ represents the market price of volatility risk, and must be independent of the particular asset. Heston (1993) specifies that $\phi = \lambda\nu$ for some constant λ, so $\kappa(\theta - \nu) - \lambda\nu$ is the risk-neutral drift rate. Recall that the risk-neutral drift of the underlying asset is r and not μ. When it comes to pricing derivatives, it is the risk-neutral drift that matters and not the real drift, whether it is the drift of the asset or of the volatility.

Thus, in the risk neutral probabilities Heston model is presented as follows:

$$\begin{aligned} dS(t) &= rS(t)dt + \sqrt{\nu(t)}S(t)d\tilde{W}_1, \\ d\nu(t) &= \bar{\kappa}(\bar{\theta} - \nu(t))dt + \sigma S(t)d\tilde{W}_2, \\ d\tilde{W}_1 d\tilde{W}_2 &= \rho dt, \end{aligned} \tag{13}$$

$$\bar{\kappa} = \kappa + \lambda, \quad \bar{\theta} = \frac{\kappa\theta}{\kappa + \lambda}. \tag{14}$$

When the contingent claim is an European vanilla put option with strike price E and maturity at T, the function $U(S, \nu,)$ satisfies the PDE (12) subject to the following boundary conditions:

$$U(S, \nu, T) = max(E - S, 0), \tag{15}$$

$$U(0, \nu, t) = E, \tag{16}$$

$$\frac{\partial U}{\partial S}(\infty, \nu, t) = -1, \tag{17}$$

$$\frac{\partial U}{\partial t}(S, 0, t) + rS\frac{\partial U}{\partial S}(S, 0, t) + \kappa\theta\frac{\partial U}{\partial \nu}(S, 0, t) - rU = 0, \tag{18}$$

$$U(S, \infty, t) = 0. \tag{19}$$

In our problem, the contingent claim is an American put option, so, as we have said, we must add a penalty term $f(E, S, U)$ equal to (10) that push up the option value $U(S, \nu, t)$ to the payoff function for avoid arbitrages opportunities.

$$\frac{\partial U}{\partial t} + \frac{1}{2}\nu S^2 \frac{\partial^2 U}{\partial S^2} + \rho\sigma\nu S \frac{\partial^2 U}{\partial S \partial \nu} + \frac{1}{2}\sigma^2 \nu \frac{\partial^2 U}{\partial \nu^2} + rS\frac{\partial U}{\partial S} + \bar{\kappa}(\bar{\theta} - \nu)\frac{\partial U}{\partial \nu} - rU + f(E, S, U) = 0, \quad (20)$$

$$0 < S < \infty, \quad 0 < \nu < \infty, \quad 0 \leq t < T. \quad (21)$$

For the writing of this section I have consulted the previous citations and Gatheral (2006), Wong and Heyde (2006), Pascucci (2011) and Wilmott (2006).

1.3 Option pricing under stochastic volatility

There are some approaches for this kind of problems, such a tree-based method Vellekoop and Nieuwenhuis (2009), PSOR method Cryer (1971), sparse wavelet Hilber et al. (2005) or finite-difference methods. As we have said earlier, our problem is summarized in solve the PDE (20) subject to the boundary conditions (15) to (19).

Note that (20) is a time dependent two-dimensional Diffusion-Advection-Reaction (DAR) equation that includes mixed spatial derivative. Dealing with finite-difference methods, the presence of this cross-derivatives involves the existence of negative coefficient terms into the numerical scheme and deteriorates the quality of the numerical solution. Details at the introduction of Zvan et al. (2003). Furthermore, finite difference schemes in the presence of a mixed spatial derivative produces four more terms in the numerical scheme with the corresponding additional computational cost and possible rounding accumulation error.

For this reasons it seems appropriate transform the problem in order to remove cross derivatives, however, as it is said in the introduction Zvan et al. (2003): "Such transformations do not appear to be possible". Despite the previous words, a section of this work addresses to remove this cross-derivatives in (20) by means of the classical technique for the reduction of second-order linear PDE in two variables to canonical form. This transformation have consequences, the problem domain changes and some considerations must be taken into account.

Once we have achieve it, we derive a pure DAR equation with the transformed boundary conditions. Only in some particular cases it is possible to solve the DAR equations exactly, as in Cokca (2003). For a more general situation, numerical techniques are required and one common methods is the semi-discretization or also known as Method Of Lines (MOL). This method lies in discretize the spatial derivatives leaving alone time derivatives and this leads to a system of Ordinary Differential Equations (ODE) that must be solved numerically. There are many methods available, such as Runge–Kutta Calvo et al. (2001) or the further time discretization deriving many types of finite difference schemes Hundsdorfer and Verwer (2003); Kaya (2015); Macías-Díaz and Puri (2012).

An alternative approach, used in this work, is the exact integration of the ODE system using the Exponential Time Differencing method (ETD), Cox and Matthews (2002), Company et al. (2018). ETD scheme results in an integral term that needs to be approximated because it is expressed in terms of the unknown solution of the semi-discretized system of ODEs, that it has been recently treated in de la Hoz and Vadillo (2016). This approach has to afford the computation challenge of the inverse matrices, not always well conditioned when eigenvalues are close to zero, Kassam and Trefethen (2005).

When we are dealing with numerical finite difference methods, even the best model may be wasted with careless analysis, so it is convenient to study the numerical solution stability as all the stepsizes tend to zero. However, while the spatial stepsize tends to zero the matrix dimension of the semi-discretized system of ODE grows without end, becoming a mathematical challenge. Apart from the stability, positivity of the solutions is also a necessary requirement because they represent prices, so guarantee it is another challenge too.

In this study a MOL method to solve (20), subject to (15)-(19), is presented together with a ETD scheme. About this last, to avoid the computation of inverse matrices, that arise from solving the ODE system integral term, we use the accurate Simpson's rule. Furthermore, taking advantage of logarithmic matrix norm and exponential matrix properties a stability and positivity analysis is performed to guarantee conditionally the boundedness of the solution independently of the semi-discrete system step-size.

2 Transformation of the problem

Firstly, we reformulate the problem with the new variable

$$\tau = T - t, \tag{22}$$

obtaining the following PDE

$$\frac{\partial U}{\partial \tau} = \frac{1}{2}\nu S^2 \frac{\partial^2 U}{\partial S^2} + \rho\sigma\nu S \frac{\partial^2 U}{\partial S \partial \nu} + \frac{1}{2}\sigma^2 \nu \frac{\partial^2 U}{\partial \nu^2} + rS\frac{\partial U}{\partial S} + \bar{\kappa}(\bar{\theta} - \nu)\frac{\partial U}{\partial \nu} - rU + f(E, S, U). \tag{23}$$

Option pricing problems have the payoff as a final condition for $t = T$. With τ we emphasize the time remaining until expiration. Now, the problem has the payoff as initial condition, that is when $\tau = 0$. We want obtain solutions at the present moment, that is when $\tau = T$. So, for an American put option value $U(S, \nu, \tau)$ we have the new boundary condition instead of (15):

$$U(S, \nu, 0) = max(E - S, 0). \tag{24}$$

2.1 Motivation

Recently, the authors Casabán et al. (2011); Company et al. (2009, 2010) used space-centered forward in time explicit finite difference schemes for the computation and numerical analysis of several one-dimensional option pricing problems. Following these ideas for the two-dimensional problem (23) on gets the following:

$$U(S_i,\nu_j,\tau^n) \approx u_{i,j}^n, \tag{25}$$
$$\frac{\partial U}{\partial \tau}(S_i,\nu_j,\tau^n) \approx \frac{u_{i,j}^{n+1}-u_{i,j}^n}{k}, \tag{26}$$
$$\frac{\partial U}{\partial S}(S_i,\nu_j,\tau^n) \approx \frac{u_{i+1,j}^n-u_{i-1,j}^n}{2h_1}; \tag{27}$$
$$\frac{\partial U}{\partial \nu}(S_i,\nu_j,\tau^n) \approx \frac{u_{i,j+1}^n-u_{i,j-1}^n}{2h_2}, \tag{28}$$
$$\frac{\partial^2 U}{\partial S^2}(S_i,\nu_j,\tau^n) \approx \frac{u_{i-1,j}^n-2u_{i,j}^n+u_{i+1,j}^n}{h_1^2}, \tag{29}$$
$$\frac{\partial^2 U}{\partial \nu^2}(S_i,\nu_j,\tau^n) \approx \frac{u_{i,j-1}^n-2u_{i,j}^n+u_{i,j+1}^n}{h_2^2}, \tag{30}$$
$$\frac{\partial^2 U}{\partial S\partial \nu}(S_i,\nu_j,\tau^n) \approx \frac{u_{i+1,j+1}^n+u_{i-1,j-1}^n-u_{i-1,j+1}^n-u_{i+1,j-1}^n}{4h_1h_2}, \tag{31}$$

where $\tau^n = nk,\ S_i = ih_1,\ \nu_j = jh_2,\ k = \Delta\tau,\ h_1 = \Delta S,\ h_2 = \Delta\nu.$

Discretizing (23) when the penalty term is active ($U < E-S$), one achieves the following scheme:

$$\begin{aligned} u_{i,j}^{n+1} =& \lambda(E-S_i) \ + \ u_{i,j}^n\Big(1-k(\lambda+r)-\frac{k}{h_1^2}\nu_j S_i^2-\frac{k}{h_2^2}\nu_j\sigma^2\Big) \\ &+ u_{i+1,j}^n\Big(\frac{\nu_j S_i}{h_1^2}+\frac{r}{h_1}\Big)\frac{k}{2}S_i \ + \ u_{i-1,j}^n\Big(\frac{\nu_j S_i}{h_1^2}-\frac{r}{h_1}\Big)\frac{k}{2}S_i \\ &+ u_{i,j+1}^n\Big(\frac{\sigma^2\nu_j}{h_2^2}+\frac{\bar\kappa(\bar\theta-\nu_j)}{h_2}\Big)\frac{k}{2} \ + \ u_{i,j-1}^n\Big(\frac{\sigma^2\nu_j}{h_2^2}-\frac{\bar\kappa(\bar\theta-\nu_j)}{h_2}\Big)\frac{k}{2} \\ &+ \frac{k}{4h_1h_2}\rho\sigma\nu_j S_i\Big(u_{i+1,j+1}^n+u_{i-1,j-1}^n-u_{i-1,j+1}^n-u_{i+1,j-1}^n\Big) \end{aligned} \tag{32}$$

Note that in the last term of the right hand side of the scheme (32) there are two negative coefficients. This is so bad for our numerical scheme because we cannot guarantee that this negativity spreads all the scheme. Remember that schemes are recursive methods, therefore if we achieve a negative value our solution will be infected and we cannot allow this because we are talking about prices. Furthermore, the coefficients that multiply the parenthesis do not allow us ensure the positivity with some condition for the step-sizes. This fact motivates the transformation of (23) into an equivalent one where the mixed spatial derivatives term disappears.

2.2 The new variables

As we have said in the introduction, following the classical techniques for reduction of second order linear PDE in two independent variables to canonical form, see for instance (Garabedian, 1998, chapter 3), we proceed to classify the right-hand side of (23) by the discriminant sign:

$$\Delta = B^2-4AC = \sigma^2\nu^2S^2(\rho^2-1), \tag{33}$$
$$B = \rho\sigma\nu S, \quad A = \frac{1}{2}\nu S^2, \quad C = \frac{1}{2}\nu\sigma^2. \tag{34}$$

Assuming correlated variables with $-1 < \rho < 1$, right side of (23) becomes of elliptic type and the suitable substitution for eliminating the mixed spatial derivative term is given by solving the following ordinary differential equation where $A = a,\ B = 2b,\ C = c$:

$$\frac{d\nu}{dS} = \frac{b + i\sqrt{ac - b^2}}{a} = \frac{\sigma\left(\rho + i\sqrt{1-\rho^2}\right)}{S} = \frac{\sigma(\rho + i\tilde{\rho})}{S}, \tag{35}$$

$$\tilde{\rho} = \sqrt{1-\rho^2}. \tag{36}$$

Solving (35) one gets:

$$d\nu = \sigma(\rho + i\tilde{\rho})\frac{dS}{S}, \tag{37}$$

$$\nu + Z_0 = \sigma(\rho + i\tilde{\rho})lnS. \tag{38}$$

And the integration constant Z_0 is related to the new variables by

$$Z_0 = y + ix. \tag{39}$$

Hence, from (38) and (39) we achieve to our new variables:

$$x = \tilde{\rho}\sigma lnS, \quad y = \rho\sigma lnS - \nu. \tag{40}$$

Now, we can express (23) with the new variables x and y by the chain rule. Denoting $U(S,\nu,\tau) = P(x,y,\tau)$ we derive the following equivalent PDE:

$$\frac{\partial P}{\partial \tau} = \frac{1}{2}\tilde{\rho}^2\sigma^2\nu\left(\frac{\partial^2 P}{\partial x^2} + \frac{\partial^2 P}{\partial y^2}\right) + \tilde{\rho}\sigma\left(r - \frac{1}{2}\nu\right)\frac{\partial P}{\partial x} + \left(\rho\sigma\left(r - \frac{1}{2}\nu\right) - \bar{\kappa}(\bar{\theta} - \nu)\right)\frac{\partial P}{\partial y} - rP + f(E,S,P). \tag{41}$$

Where, now, $f(E,S,P)$ is:

$$f(E,S,P) = \lambda\ max(E - e^{\frac{x}{\tilde{\rho}\sigma}} - P,\ 0). \tag{42}$$

We want to remark that the previous substitution not only allows us to ensure positivity but also has computational advantages. The elimination of cross derivatives simplify our scheme because the stencil has now five points and not nine. See Figure 4

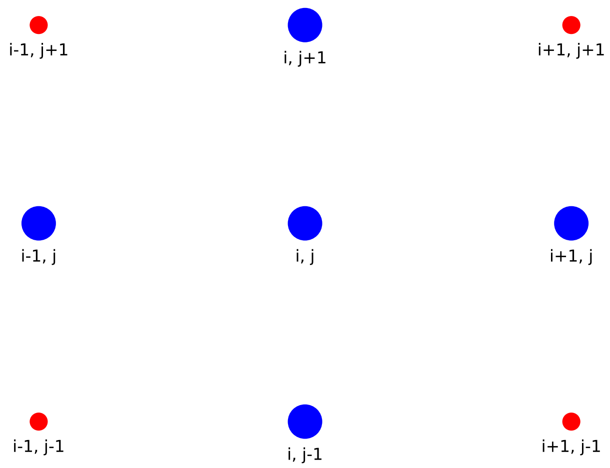

Figure 4: Five-point versus nine-point stencils

2.3 Artificial Boundary conditions

Now, we should show the new boundary conditions of the transformed problem, but it will not be necessary. Inside a bounded domain, the PDE numerical solution will not be crucially affected by artificial boundary conditions, then some simplified strategies can be taken into consideration, see (Jaillet et al., 1990, proposition 4.1). In this work we choose the artificial boundary conditions at the bounded numerical domain boundaries to be equal to the values at $\tau = 0$, i.e. the payoff function, for more see Kovalov et al. (2007). Explicitly:

$$\lim_{S\to 0} U(S,\nu,\tau) = E, \tag{43}$$

$$\lim_{S\to \infty} U(S,\nu,\tau) = 0, \tag{44}$$

$$\lim_{\nu\to 0} U(S,\nu,\tau) = max(E-S,0), \tag{45}$$

$$\lim_{\nu\to \infty} U(S,\nu,\tau) = max(E-S,0). \tag{46}$$

We have decided this boundary conditions but other authors as Zhu and Chen (2011) choose another ones different:

$$\lim_{\nu\to 0} U(S,\nu,t) = 0, \quad \lim_{\nu\to \infty} U(S,\nu,t) = E. \tag{47}$$

And other authors as Yousuf and Khaliq (2013) or Düring and Pitkin (2019) use another one. Typically there are a combination of Neumann boundary conditions. The choice of one or other set of boundary conditions it is not crucial, the critical fact is that the limits are very far from the area where we want to obtain solutions.

2.4 Domain assumptions

Note that ν from (40) takes the expression in terms of x and y as follows:

$$\nu = \frac{\rho}{\tilde{\rho}} x - y. \tag{48}$$

The previous expression is very relevant because specifies a relationship between ν and the new variables. This means that, for a given ν, the new variables are related by a linear equation, with $\rho/\tilde{\rho}$ as slope and ν as vertical intercept. Thus, the problem transformation changes the domain, from a square to rhomboid domain and this linear relation is the reason. It is also relevant that this expression shows us the relation between x and y:

$$\frac{\Delta y}{\Delta x} = m, \quad m = \frac{\rho}{\tilde{\rho}}. \tag{49}$$

The domain defined at (21) has been changed by the new variables (40). So the domain of the transformed problem for variables x and τ is:

$$-\infty < x < +\infty, \quad 0 < \tau \leq T. \tag{50}$$

Remember that ν means the underlying asset variance, so it has to be positive and to ensure that we achieve from (48) the expression $(\rho/\tilde{\rho})x - y > 0$. Hence, to ensure this positivity the variable y must be upper bounded:

$$-\infty < y < mx. \tag{51}$$

Thus the domain of the transformed problem is as follows:

$$D = \{(x, y, \tau);\ x \in \mathbb{R},\ y < mx,\ 0 < \tau \leq T\}. \tag{52}$$

It is easy to see that our new domain (52) is not bounded, so an exact numerical calculus is impossible. Then, for obtain solutions to the PDE (41), we must choose a bounded numerical domain where we can solve the PDE by approximations with finite differences. Working with the original variables, we must choose a rectangle $[S_1, S_2] \times [\nu_1, \nu_2]$. With S_1 and ν_1 close to zero and S_2 and ν_2 far enough from zero, see Kangro and Nicolaides (2000).

Remark 1. Because of the spatial variables transformation (40) a rectangle $[S_1, S_2] \times [\nu_1, \nu_2]$ is transformed into rhomboid $\overline{ABCD}$ where the sides are described by the following:

$$
\begin{aligned}
\overline{AD} &= \Big\{(x,y) \in \mathbb{R}^2 \mid x = a = \tilde{\rho}\sigma lnS_1,\ y = ma - \nu,\ \nu_1 \le \nu \le \nu_2\Big\}, \\
\overline{AB} &= \Big\{(x,y) \in \mathbb{R}^2 \mid a \le x \le b = \tilde{\rho}\sigma lnS_2,\ y = mx - \nu_2,\ \Big\}, \\
\overline{BC} &= \Big\{(x,y) \in \mathbb{R}^2 \mid x = b,\ y = mb - \nu,\ \nu_1 \le \nu \le \nu_2\Big\}, \\
\overline{CD} &= \Big\{(x,y) \in \mathbb{R}^2 \mid a \le x \le b,\ y = mx - \nu_1\Big\}. \qquad (53)
\end{aligned}
$$

Remark 2. In case S and ν are fully correlated: $|\rho| = 1$. From (33) the discriminant $\Delta = 0$ and the right side of (23) become a parabolic PDE. Following the techniques for reduction to canonical form, an appropriate substitution is $x = S$; $y = \nu - \rho\sigma$ nd the transformed equation takes the following form:

$$
\frac{\partial P}{\partial \tau} = \frac{1}{2}\nu x^2 \frac{\partial^2 P}{\partial x^2} + rx\frac{\partial P}{\partial x} + \left(\sigma\rho\left(\frac{1}{2}\nu - r\right) - \bar{\kappa}(\bar{\theta} - \nu)\right)\frac{\partial P}{\partial y} + f(E,S,P) \qquad (54)
$$

3 Semi-discretization and ETD scheme

In this section we are going to define the relations between the differents step-sizes of the discretizations and the numerical methods developed to propose a solution to the problem.

3.1 Discretization

Using the classical step-size discretizations, the transformation (40) and Remark 1, we use a discretization where the step-sizes of x and y are related by m.

In accordance with (53) we discretize the variable x

$$
\begin{aligned}
&x_i \in [a,b],\ \ h = \Delta x,\ \ N_x = \frac{b-a}{h}, \\
&x_i = a + ih,\ \ 0 \le i \le N_x \qquad (55)
\end{aligned}
$$

variable y

$$
y_{ij} \in [y_1 = mx - \nu_1,\ y_2 = mx - \nu_2],\ \ mh = \Delta y,\ \ N_y = \frac{y_1 - y_2}{mh} = \frac{\nu_2 - \nu_1}{mh}. \qquad (56)
$$

Let us denote

$$y_0 = ma - \nu_2. \qquad (57)$$

The first element of each row is:

$$y_{i0} = y_0 + (x_i - a)m = y_0 + imh. \qquad (58)$$

Then, all the mesh-points with the same i index are:

$$y_{ij} = y_0 + (i+j)mh, \quad 0 \le j \le N_y. \qquad (59)$$

And we discretize τ

$$\tau^n = kn, \quad 0 \leq n \leq N_\tau, \quad \Delta\tau = k = \frac{T}{N_\tau}. \tag{60}$$

Thus, we guarantee that the numerical rhomboid domain includes all the mesh-points of the discretization. Now, the rhomboid boundary sides are partitioned in the following way:

$$\begin{aligned}
P(\overline{AB}) &= \{(x_i, y_{i0}) \mid 0 \leq i \leq N_x, \;\; j = 0\}\,, \\
P(\overline{BC}) &= \{(x_{N_x}, y_{N_x j}) \mid i = N_x, \;\; 0 \leq j \leq N_y\}\,, \\
P(\overline{CD}) &= \{(x_i, y_{iN_y}) \mid 0 \leq i \leq N_x, \;\; j = N_y\}\,, \\
P(\overline{AD}) &= \{(x_0, y_{0j}) \mid i = 0, \;\; 0 \leq j \leq N_y\}\,.
\end{aligned} \tag{61}$$

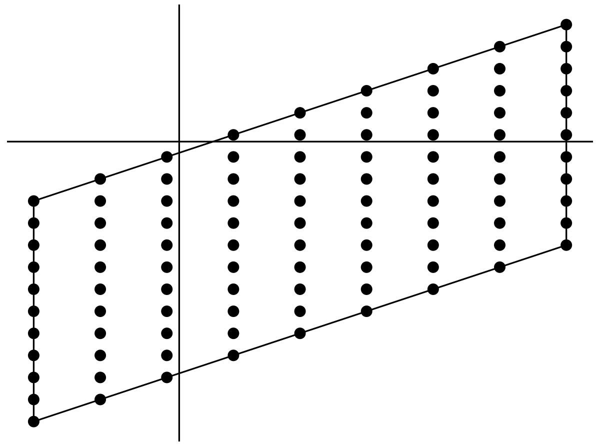

Figure 5: Rhomboid domain

Let us denote the set of all mesh points by Γ, the subset located at the numerical domain boundary by $\partial\Gamma$ and the interior nodes by $\dot{\Gamma} = \Gamma - \partial\Gamma$.

3.2 New variable

For these mesh-points, located by their i and j value, we can create a new variable that depends of both previous variables.

$$\xi_D = (x_i, y_j). \tag{62}$$

Henceforth we denote y_{ij} as y_j if the i value is defined previously by x_i. All the mesh-points ξ involve the combinations of x_i and y_j, so ξ is related with the total number of points and the variables i and j. For each pair of indices $[i, j]$ the index D is

$$D = (N_y + 1)i + j, \quad 0 \leq i \leq N_x, \quad 0 \leq j \leq N_y. \tag{63}$$

The total number $N+1$ of points ξ in the mesh-grid is

$$N + 1 = (N_y + 1)(N_x + 1). \tag{64}$$

Then, the index D defined by (63) takes $N+1$ integer values, $0 \leq D \leq N$. Order in the set of mesh points ξ is established by (63) in the following way:

$$\begin{array}{ll|ll|c|ll}
D = 0 & (0,0) & D = N_y + 1 & (1,0) & & D = N_x(N_y+1) & (N_x, 0) \\
D = 1 & (0,1) & D = N_y + 2 & (1,1) & & D = N_x(N_y+1) + 1 & (N_x, 1) \\
D = 2 & (0,2) & D = N_y + 3 & (1,2) & \dots & D = N_x(N_y+1) + 2 & (N_x, 2) \\
\vdots & \vdots & \vdots & \vdots & & \vdots & \vdots \\
D = N_y & (0, N_y) & D = 2N_y + 1 & (1, N_y) & & D = (N_y+1)(N_x+1) & (N_x, N_y)
\end{array}$$

If we have an arbitrary ξ_D, taking into account (63), value we can recover the x_i and y_j corresponding values with the quotient and rest of a division:

$$\begin{array}{cc} D & \underline{|N_y + 1} \\ i & j \end{array} \tag{65}$$

Henceforth, for given point ξ_D, we define the recovered points as x_D and y_D. We derive x_D by (55):

$$x_D = a + E\left[\frac{D}{N_y + 1}\right] h, \tag{66}$$

where $E[\cdot]$ means the integer part of $\frac{D}{N_y+1}$ division. Knowing that $j = D - (N_y + 1)i$ by we derive an expression for y_D from (56):

$$y_D = ma - \nu_2 + \left(D + E\left[\frac{D}{N_y + 1}\right] - (N_y + 1)E\left[\frac{D}{N_y + 1}\right]\right) mh. \tag{67}$$

We can also derive an expression for ν_D from (48):

$$\nu_D = \nu_2 - jmh. \tag{68}$$

3.3 Derivatives

Once we have defined ξ_D and we know recover x_i, y_j and ν_D we can approximate the spatial derivatives of (41) using centered differences approximations and ξ_D.

Knowing that that $P(x, y, \tau) = P(\xi_D, \tau)$ and that derivatives for a given function $f(x)$ and variable x can be approximated by:

$$\frac{\partial f}{\partial x} \approx \frac{f(x+h) - f(x-h)}{2h}, \quad \frac{\partial^2 f}{\partial x^2} \approx \frac{f(x+h) - 2f(x) + f(x-h)}{h^2}.. \tag{69}$$

We can write the derivatives that involves x and y of (41) with ξ_D. If we are moving over the x-axis, ξ_D is affected increasing D around N_y, and over y-axis, ξ_D increases only one point. Therefore we can derive the derivatives approximations, omitting τ argument, as follows:

$$\frac{\partial^2 P}{\partial x^2}(\xi_D) \approx \frac{P(\xi_{D+N_y}) - 2P(\xi_D) + P(\xi_{D-N_y})}{h^2}, \tag{70}$$

$$\frac{\partial^2 P}{\partial y^2}(\xi_D) \approx \frac{P(\xi_{D+1}) - 2P(\xi_D) + P(\xi_{D-1})}{(mh)^2}, \tag{71}$$

$$\frac{\partial P}{\partial x}(\xi_D) \approx \frac{P(\xi_{D+N_y}) - P(\xi_{D-N_y})}{2h}, \tag{72}$$

$$\frac{\partial P}{\partial y}(\xi_D) \approx \frac{P(\xi_{D+1}) - P(\xi_{D-1})}{2mh}. \tag{73}$$

Applying (70)-(73) to (41) and denoting $P(\xi_{D\pm z})$ as $P_{D\pm z}$ we achieve the following system of Ordinary Differential Equations (ODE):

$$\begin{aligned}\frac{\partial P}{\partial \tau}(\xi_D) = &\left(-\frac{2\alpha_D}{h^2} - \frac{2\alpha_D}{(mh)^2} - r\right) P_D + \left(\frac{\alpha_D}{(mh)^2} + \frac{\gamma_D}{mh}\right) P_{D+1} + \left(\frac{\alpha_D}{(mh)^2} - \frac{\gamma_D}{mh}\right) P_{D-1} \\ &+ \left(\frac{\alpha_D}{h^2} + \frac{\beta_D}{h}\right) P_{D+N_y} + \left(\frac{\alpha_D}{h^2} - \frac{\beta_D}{h}\right) P_{D-N_y} + f(P_D),\end{aligned} \tag{74}$$

Where

$$\alpha_D = \frac{1}{2}\tilde{\rho}^2\sigma^2\nu_D \tag{75}$$

$$\beta_D = \frac{1}{2}\tilde{\rho}\sigma\left(r - \frac{1}{2}\nu_D\right) \tag{76}$$

$$\gamma_D = \frac{1}{2}\left(\rho\sigma\left(r - \frac{1}{2}\nu_D\right) - \bar{\kappa}(\bar{\theta} - \nu_D)\right) \tag{77}$$

3.4 System of ODEs

The previous system (74) can be presented in the following vectorial form

$$\frac{dP}{d\tau} = A(\xi)P(\tau) + f(\xi, P). \tag{78}$$

Where $P = P(\tau) \in R^{N+1}$ denotes the vector of all values $P_0, \cdots, P_N$, such that $P = [P_0, \ldots, P_N]^T$ and $f(\xi, P) = [f_0, \ldots, f_N]^T$ is the penalty term vector for every P_D. Matrix $A(\xi) = (a_{DL})_{D,L=0}^N \in \mathbb{R}^{(N+1)\times(N+1)}$ is a singular matrix whose non-zero entries are

$$\left.\begin{array}{l} a_{D,D} = -\left(\frac{2\alpha_D}{h^2} + \frac{2\alpha_D}{(mh)^2} + r\right) \\ a_{D,D\pm 1} = \frac{\alpha_D}{(mh)^2} \pm \frac{\gamma_D}{mh} \\ a_{D,D\pm N_y} = \frac{\alpha_D}{h^2} \pm \frac{\beta_D}{h} \end{array}\right\} \text{if } \xi_D \in \dot{\Gamma}. \tag{79}$$

Note that the rows of $A(\xi)$ corresponding to boundary points $\xi_D \in \partial\Gamma$ are zero rows.

denoting $f(\xi, P)_D$ as the Dth element of vector $f(\xi, P)$, one gets

$$f(\xi, P)_D = \begin{cases} 0 & \text{if } \xi_D \in \partial\Gamma \\ f(P_D) & \text{if } \xi_D \in \dot{\Gamma} \end{cases}. \tag{80}$$

Matrix $A(\xi) \in \mathbb{R}^{(N+1)\times(N+1)}$ dimension depends on h:

$$(N+1) = (N_x+1)(N_y+1) = \left(\frac{b-a}{h} + 1\right)\left(\frac{\nu_2 - \nu_1}{mh} + 1\right) = O\left(\frac{1}{h^2}\right) \to \infty, \quad h \to 0. \tag{81}$$

The previous system (78) is equivalent to a non-linear integral equation (semigroups approach, see Pazy (1983)):

$$P(\tau) = e^{A(\tau-\tau_0)}P(\tau_0) + \int_{\tau_0}^{\tau} e^{A(\tau-v)} f(\xi, P(v))\, dv, \quad \tau > \tau_0. \tag{82}$$

3.5 ETD method

The Exponential Time Differencing (ETD) method, see Cox and Matthews (2002), lies in develop numerical methods to solve (82). It is now when we introduce the temporal discretization defined in (60). For each sub-interval $\left[t^n, t^{n+1}\right]$ of length k, we approximate:

$$P(\tau^{n+1}) = e^{Ak}P(\tau^n) + \int_{\tau^n}^{\tau^{n+1}} e^{A(\tau^{n+1}-v)} f(\xi, P(v))\, dv. \tag{83}$$

And now, with the new variable $s = t^{n+1} - v$, we achieve:

$$P(\tau^{n+1}) = e^{Ak}P(\tau^n) + \int_0^k e^{As} f(\xi, P(\tau^{n+1} - s))\, ds. \tag{84}$$

This exact solution is given by Cox and Matthews (2002)[Section 2.1]. Note that the solution is also function of himself, therefore we need to make some assumptions to provide solutions.

Company et al. (2018) propose a first explicit integral approximation by replacing $P(\tau^{n+1} - s)$ by the known value $P(\tau^n)$ corresponding to $s = k$:

$$P(\tau^{n+1}) = e^{Ak}P(\tau^n) + \left(\int_0^k e^{As}ds\right) f(\xi, P(\tau^n)) \tag{85}$$

In accordance with Cox and Matthews (2002)[Section 2.1] the local truncation error is $O(k^2)$.

It is well known that when A is a regular matrix, $\int_0^k e^{As}ds = A^{-1}\left(e^{Ak} - I\right)$ but this exact solution can be problematic because of A^{-1} calculus. A matrix can be singular or ill-conditioned in this kind of problems (as ours) therefore $\nexists A^{-1}$ but $\int_0^k e^{As}ds$ exists. So, instead of solving the integral, we use the accurate Simpson's rule, see Atkinson (1989).

$$\int_0^k e^{As}ds = k\varphi(A,k) + O(k^5), \quad \varphi(A,k) = \frac{1}{6}\left(I + 4e^{A\frac{k}{2}} + e^{Ak}\right). \tag{86}$$

Letting us denote $P(\tau^n)$ as P^n we propose the numerical solution to (41) by the following scheme:

$$P^{n+1} = e^{Ak}P^n + k\ \varphi(A,k)\ f(\xi, P^n). \tag{87}$$

4 Positivity and stability

In this section we pay attention to the scheme stability and positivity, i.e. that the numerical solution P^n remains bounded at each point.

Letting us denote the infinite vector norm as:

For $v \in \mathbb{R}^n$,

$$\parallel v \parallel_\infty = \max_n\ |v_n|. \tag{88}$$

We are going to show that $\parallel P^n \parallel_\infty \leq E,\ 0 \leq n \leq N_t$, where E (the strike price) is independent of the spatial and temporal step-size h and k, and that for each level n also $P^n \geq 0$. For the proposed scheme, stability analysis is a challenging task, because the matrix A dimension grows as step-sizes decrease.

The positivity can be assured if all the matrix elements of e^{Ak} and $\varphi(A,k)$ are positives. Before starting and for the sake of clarity, in this work we recall some definitions and results that might be found in Kaczorek (2002). A matrix $A \in \mathbb{R}^{n\times n}$ is called Metzler if its off-diagonal elements are non-negative i.e. $a_{i,j} \geq 0,\ 1 \leq i \neq j \leq n$.

If A is Metzler, then $e^{At} \geq 0$ for $t \geq 0$. It can be showed taking $a_0 = \min_D\ a_{D,D}$:

$$\begin{aligned} & e^{A} = e^{a_0 I}\, e^{A-a_0 I} \geq 0, \text{ because} \\ & e^{a_0 I} = I\, e^{a_0} \geq 0 \text{ and} \\ & e^{A-a_0 I} \geq 0. \end{aligned} \tag{89}$$

4.1 Positivity

Hence if we demonstrate that our matrix A is Metzler, we can assure that $e^{At} \geq 0$ and $\varphi(A,k) \geq 0$. To do it, we take $a_{D,D\pm 1}$ and $a_{D,D\pm N_y}$ from (79) and we study how they change with h. If the stepsize h is rightly select the coefficients will be positive, and A will be Metzler:

$$a_{D,D\pm 1} = \frac{1}{mh}\left(\frac{\alpha_D}{mh} \pm \gamma_D\right), \quad a_{D,D\pm N_y} = \frac{1}{h}\left(\frac{\alpha_D}{h} \pm \beta_D\right), \tag{90}$$

$$a_{D,D\pm 1} \geq 0 \Rightarrow \begin{cases} \frac{\alpha_D}{mh} + \gamma_D \geq 0 \\ \frac{\alpha_D}{mh} - \gamma_D \geq 0 \end{cases} \begin{cases} -\alpha_D \leq mh\gamma_D \\ \alpha_D \geq mh\gamma_D \end{cases}, \tag{91}$$

$$-\alpha_D \leq mh\gamma_D \leq \alpha_D, \quad mh\,|\gamma_D| \leq \alpha_D, \quad h \leq \frac{\alpha_D}{m\,|\gamma_D|}. \tag{92}$$

$$\text{Analogously, } a_{D,D\pm N_y} \geq 0 \Rightarrow h \leq \frac{\alpha_D}{|\beta_D|}. \tag{93}$$

We can combine both conditions to h by

$$\beta = \max_D\ |\beta_D|, \quad \gamma = \max_D\ |\gamma_D|, \quad \alpha = \min_D\ \alpha_D = \frac{1}{2}\tilde{\rho}^2\sigma^2\nu_1, \tag{94}$$

$$\delta = \max\{\beta,\ m\gamma\}, \tag{95}$$

$$h \leq \frac{\alpha}{\delta}. \tag{96}$$

Therefore taking an h that satisfy (96) we are in position to affirm that the numerical solution positivity is guaranteed.

4.2 Some definitions and properties

Before talking about the stability we should explain some concepts. It is well known that the exponential matrix norm is bounded by the exponential of logarithmic norm $\mu[A]$, see Dahlquist (1961):

$$\|\, e^{Ak} \,\| \leq e^{k\mu[A]}. \tag{97}$$

Denoting the real part of a complex number x by $\Re(x)$, $\mu_\infty[A]$ can be calculated as follows, see C.A. Desoer (1975)[p.33],

$$\mu_\infty[A] = \max_i \left(\Re(a_{ii}) + \sum_{j\neq i}^{n} |a_{ij}| \right). \tag{98}$$

Knowing the coefficients of matrix A and their sign (79), we can see that the row's sum only can have two values:

$$\sum_{j=1}^{N+1} a_{ij} = \begin{cases} 0 & \text{if } \xi_D \in \partial\Gamma \\ -r & \text{if } \xi_D \in \dot{\Gamma} \end{cases}, \quad i = 1, 2 \ \dots \ N+1. \tag{99}$$

So, from (98) one gets $\mu_\infty[A] = 0$, therefore from (97) $\| e^{Ak} \|_\infty \leq e^0 = 1$ and from (86) $\| \varphi(A,k) \|_\infty \leq 1$. We can see that matrix A has some zero rows, and their corresponding rows in e^{Ak} have only one entry equal to 1 and 0 at the others, consequently we can affirm $\| e^{Ak} \|_\infty = \| \varphi(A,k) \|_\infty \geq 1$. Then, as we have shown inequality in both directions we can affirm:

$$\| e^{Ak} \|_\infty = \| \varphi(A,k) \|_\infty = 1. \tag{100}$$

This result will be important to future discussions.

The non-negativity of P^n follows from the Metzler matrix property, that is the non-negative of e^{Ak} and by extension of $\varphi(A,k)$. The boundedness solution $P_D^n \leq E$ is proven using the induction principle.

4.3 Stability

Let us represent each row i of P^{n+1} in (87) as a function g_i with arguments $(P_0^n, \cdots, P_N^n)$

$$P_i^{n+1} = g_i(P_0^n, \cdots, P_N^n) = (e^{Ak})_i P^n + k\varphi(A,k)_i \ f(\xi, P^n), \quad 0 \leq i,j \leq N, \quad 0 \leq n \leq N_\tau. \tag{101}$$

Assuming the boundedness of the derivative $\left| \frac{\partial f(\xi_i, P)}{\partial P} \right| \leq \lambda$, $\xi_i \in \dot{\Gamma}$, $0 \leq P \leq E$, then from non-negativity of e^{Ak} and $\varphi(A,k)$ one gets

$$\frac{\partial g_i}{\partial P_j^n} \geq (e^{Ak})_{ij} - \lambda \ k \ \varphi(A,k)_{ij}, \quad 0 \leq i,j \leq N. \tag{102}$$

Letting us denote $\psi(A,k) = e^{Ak} - \lambda \ k \ \varphi(A,k)$ (lower bound derivative) and the vector function $g_i(P_0^n, \cdots, P_N^n)$ as $[g_0, \dots, g_N]^T$. Then from (102) the Jacobian matrix $\frac{\partial g}{\partial P^n}$ satisfies

$$\frac{\partial g}{\partial P^n} \geq \psi(A,k). \tag{103}$$

Note that the non-negativity of $\psi(A,k)$ guarantees the non-negativity of $\frac{\partial g}{\partial P^n}$ also, and hence, g_i increase in each direction P_j^n. Thus, the next step is verify $\psi(A,k) \geq 0$.

Under the assumption (96), $B = A - a_0 I$ verifies $B \geq 0$ in a similar way as in (89). Taking into account $e^{Ak} = e^{a_0 k} e^{Bk}$ and $e^{Bk} = I + \sum_{s=1}^{\infty} \frac{B^s k^s}{s!}$, we can develop $\psi(A,k)$ in terms of B powers and write it as

$$\psi(A,k) = \phi_0(k) + \sum_{s=1}^{\infty} \phi_s(k) \frac{B^s k^s}{s!}. \tag{104}$$

Where

$$\phi_0(k) = e^{a_0 k} - \frac{\lambda\, k}{6}\left(1 + 4e^{a_0 \frac{k}{2}} + e^{a_0 k}\right), \tag{105}$$

$$\phi_s(k) = e^{a_0 k} - \frac{\lambda\, k}{6}\left(\frac{4}{2^s} e^{a_0 \frac{k}{2}} + e^{a_0 k}\right). \tag{106}$$

Note that $\phi_s(k) > \phi_0(k)$ for $s \geq 1$, then if we show $\phi_0(k) \geq 0$ this means $\psi(A,k) \geq 0$ too. Then, by a Taylor expansion of $\phi_0(k)$, with $0 < \xi < k$, we can write

$$\phi_0(k) = \phi_0(0) + \phi_0'(0)k + \frac{\phi_0''(\xi)}{2} k^2. \tag{107}$$

Where

$$\phi_0(0) = 1, \tag{108}$$

$$\phi_0'(0) = a_0 - \lambda, \tag{109}$$

$$\phi_0''(\xi) = a_0^2 + \frac{\lambda}{3}|a_0| e^{a_0 \frac{\xi}{2}} + \frac{\lambda |a_0|}{6}(2 - |a_0|\xi)(e^{a_0 \xi} + e^{a_0 \frac{\xi}{2}}). \tag{110}$$

Note that the two first terms sum of $\phi_0(k)$ Taylor expansion is positive if $k < \frac{1}{\lambda + |a_0|}$. By (**??**) we know that $|a_0|$ is

$$|a_0| = 2\alpha_m \left(\frac{1}{h^2} + \frac{1}{(mh)^2}\right) + r \tag{111}$$

where

$$\alpha_m = \max_D \alpha_D \tag{112}$$

So, the final stability condition is

$$k \leq \frac{h^2}{(\lambda + r)h^2 + 2\alpha_m \left(\frac{1+m^2}{m^2}\right)} \tag{113}$$

Condition (113) implies $(2 - |a_0|\xi) > 0$, so $\frac{\phi_0''(\xi)}{2}k^2 > 0$. Thus, Jacobian matrix $\frac{\partial g}{\partial P^n}$ is non-negative and our scheme, initially bounded:

$$0 \leq P^0 = \left[P_0^0, \cdots, P_N^0\right]^T \leq [E, E, \cdots, E]^T. \tag{114}$$

For the sake of clarity we recall the definition of schemes $\| \cdot \|_\infty$-stable. We say that the scheme (87) is $\| \cdot \|_\infty$-stable on our domain $\Gamma \times [0, T]$ if for every domain partition we can verify:

$$\| P^n \|_\infty \leq K, \quad 0 \leq n \leq N_\tau. \tag{115}$$

For some positive constant K independent of h, k, and n.

4.4 Induction principle

Assuming $0 \leq P_i^n \leq E,\ 0 \leq i \leq N$ and conditions (113) and (96) are satisfied it is guaranteed that matrix A is Metzler and $f(\xi, P^n) \geq 0$, so $P_i^n \geq 0$. In addition, as $\frac{\partial g}{\partial P^n} \geq 0$ every g_i is increasing in each direction P_j^n: $g_i(P_0^n, \cdots, P_N^n) \leq g_i(E, \cdots, E)$:

$$\begin{aligned} P_i^{n+1} &= g_i(P_0^n, \cdots, P_N^n) = (e^{Ak})_i P^n + k\varphi(A,k)_i\ f(\xi, P^n) \\ &\leq g_i(E, \cdots, E) = (e^{Ak})_i \mathbf{E} + k\varphi(A,k)_i\ f(\xi, \mathbf{E}). \end{aligned} \tag{116}$$

where $\mathbf{E} = [E, \cdots, E]^T$.

Thus from (116) we can say

$$(e^{Ak})_i \mathbf{E} = E \sum_{j=1}^{N+1} (e^{Ak})_{ij} \overset{Metz.}{=} E \sum_{j=1}^{N+1} \left|(e^{Ak})_{ij}\right| \leq\ E \parallel e^{Ak} \parallel_\infty \leq\ E\ e^{k\mu_\infty[A]} = E, \tag{117}$$

because

$$\mu_\infty[A] = \max_i \left\{ a_{ii} + \sum_{j \neq i} |a_{ij}| \right\} = \max\{0,\ -r\} = 0 \tag{118}$$

and

$$f(\xi, \mathbf{E}) = 0. \tag{119}$$

Then,

$$P_i^{n+1} \leq E, \quad 0 \leq i \leq N, \quad 0 \leq n \leq N_\tau - 1. \tag{120}$$

And finally we get

$$\| P^n \|_\infty \leq E. \tag{121}$$

Note that we have shown not only the positivity and stability of the solution but also that the solution remain between zero and the strike price as it is expected dealing with put options.

Summarizing all above, the main result of the paper is established as follows.

Theorem 1 *With the previous notation under conditions* (96) *and* (113) *the numerical solution* P^n *of the scheme* (87) *is non-negative and* $\| \cdot \|_\infty$*-stable, with* $\| P^n \|_\infty \leq E$ *for* $0 \leq n \leq N_\tau$.

5 Numerical experiments

In this section we present numerical results for American put options with three sets of parameters. We compare it with other authors and we provide some useful discussions. The prices are presented for the asset values $S = 8, 9, 10, 11, 12$, for variance values $\nu = 0,0625;\ 0,25$ and the common parameters presented at Table 1. To obtain solutions we interpole linearly the ν values and for asset values we use a cubic spline interpolation. We also plot the numerical solutions for two sets of parameters at Figures 6 and 7.

Table 1: Common parameters

Parameters	Values
S_1	0,25
S_2	40
ν_1	0,002
ν_2	1,2
λ	200

5.1 Results comparison

Table 2: Comparison of the computed option prices under set 1

$E = 10;\ T = 0,25;\ r = 0,1;\ \kappa = 5;\ \theta = 0,16;\ \sigma = 0,9;\ \rho = 0,1$

ν value	(N_x, N_y, N_τ)	Asset values				
		8	9	10	11	12
$\nu = 0,0625$	(65, 169, 5000)	1,9941	1,1020	0,5139	0,2122	0,0843
	Yousuf and Khaliq (2013) (400,80,20)	1,9958	1,1051	0,5167	0,2119	0,0815
	Clarke and Parrott (1996)	2,00	1,108	0,5316	0,2261	0,0907
	Ikonen and Toivanen (2007) (4096,2048,4098)	2,0000	1,10763	0,52004	0,21368	0,08205
	Oosterlee (2003) (256,256)	2,000	1,107	0,517	0,212	0,0815
	Persson and von Sydow (2010) (81,21,21)	1,9976	1,10768	0,51837	0,21424	0,08193
	Zhu and Chen (2011) (100,100,50000)	2,0000	1,0987	0,5082	0,2106	0,0861
	Zvan et al. (1998) (177,103)	2,000	1,1076	0,5202	0,2138	0,0821
$\nu = 0,25$	(65, 169, 5000)	2,0744	1,3291	0,7920	0,4467	0,2437
	Yousuf and Khaliq (2013) (400,80,20)	2,0760	1,3316	0,7945	0,4473	0,2423
	Clarke and Parrott (1996)	2,0733	1,3290	0,7992	0,4536	0,2502
	Ikonen and Toivanen (2007) (4096,2048,4098)	2,0784	1,3336	0,7960	0,4483	0,2428
	Oosterlee (2003) (256,256)	2,0790	1,3340	0,7960	0,4490	0,2430
	Persson and von Sydow (2010) (81,21,21)	2,0777	1,33219	0,79377	0,44621	0,2417
	Zhu and Chen (2011) (100,100,50000)	2,0781	1,3337	0,7965	0,4496	0,2441
	Zvan et al. (1998) (177,103)	2,0784	1,3337	0,7961	0,4483	0,2428

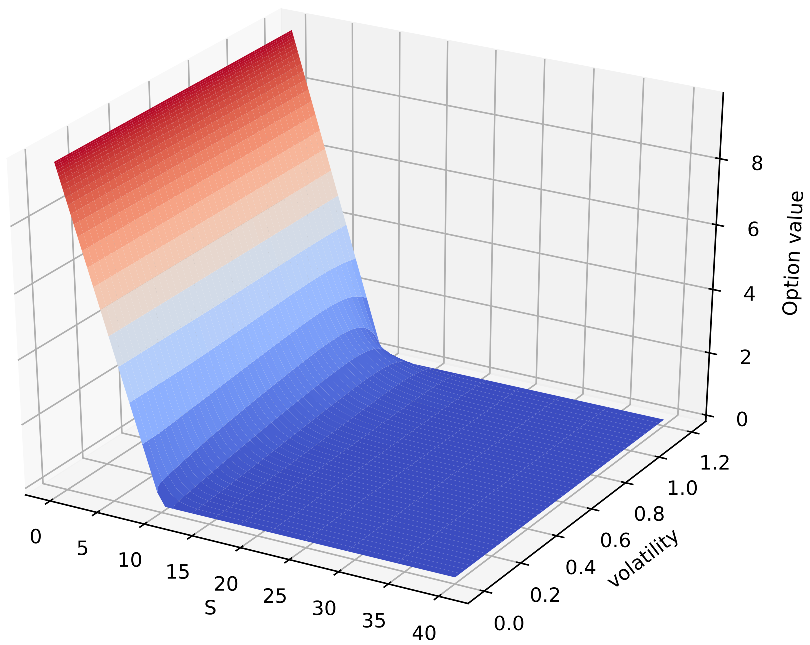

Figure 6: Numerical solutions with set 1

It can be seen at Table 2 that our results are competitive and efficient in comparison with other methods . We want to highlight that with this set of parameters (which has been used for the past thirty years) we do not take advantage of all the potential of the method. Note that $|\rho|$ is close to zero and that is a situation where the cross-derivative term $\frac{\partial^2 U}{\partial S \partial \nu}$ of (23) has not a significant influence in the numerical solution. So it looks like if our effort to remove this term is useless with this set of parameters. This fact motivates us test the method potency providing solutions with a higher $|\rho|$ that we do not found in the literature at Table 3.

Table 3: New option prices

$E = 10;\ T = 0,25;\ r = 0,1;\ \kappa = 5;\ \theta = 0,16;\ \sigma = 0,9;\ \rho = 0,7$

ν value	(N_x, N_y, N_τ)	Asset values				
		8	9	10	11	12
$\nu = 0,0625$	(150,57,2500)	2,0022	1,1382	0,5163	0,1573	0,0317
$\nu = 0,25$		2,1160	1,3665	0,7937	0,4062	0,1803

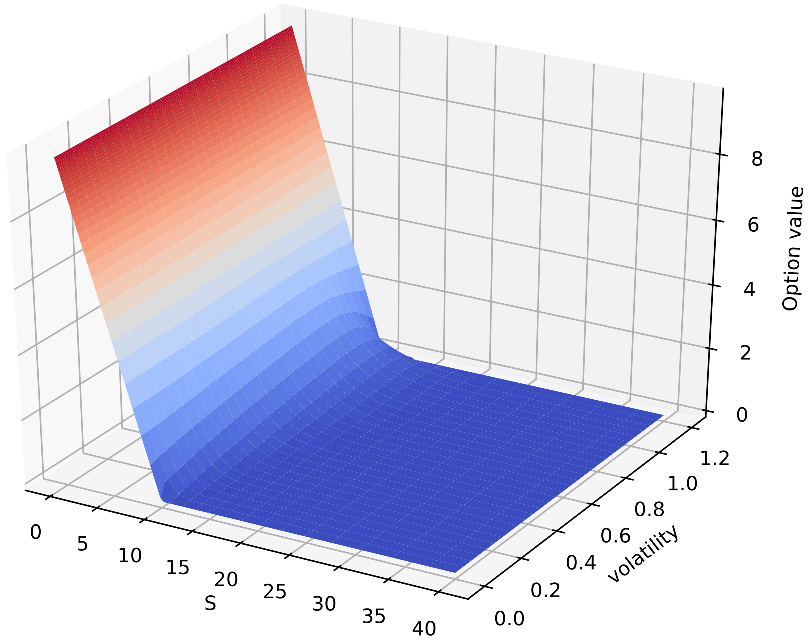

Figure 7: Numerical solutions with high $|\rho|$

5.2 Greeks

We also compute the first order greeks $\Delta = \frac{\partial P}{\partial S}$ and $\nu = \frac{\partial P}{\partial \nu}$ for the set 1 values:

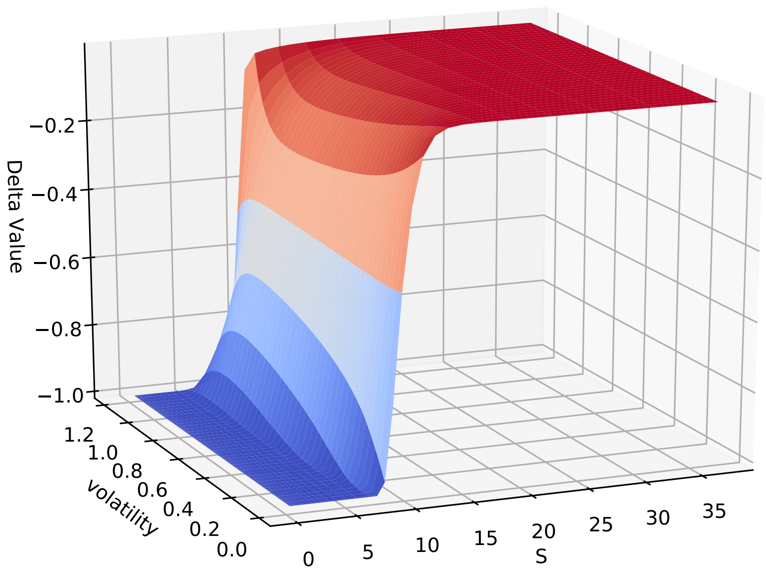

Figure 8: Δ values

As we can see Δ is, for the first S values close to -1. When S is arriving to the at the money area ($S \approx E$), Δ moves fast to zero, and then remain there for big values of S.

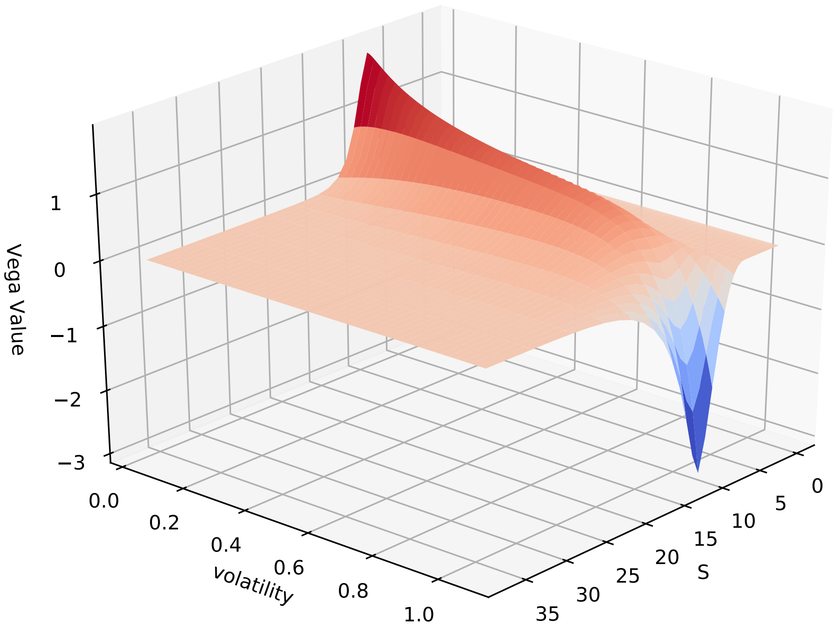

Figure 9: ν values

We can see that, in general, if we are not close to the at the money (ATM) area ν is close to zero. But in the ATM area ν is positive and progressively decays. We can see that for a big volatility values in the ATM zone $\nu \leq 0$. This is because we impose as a boundary condition the payoff function, the to converge to the payoff function that is necessary.

In general, both greeks behave as we expect.

5.3 Numerical convergence

Another important issue for a numerical scheme is the study of the numerical convergence. To study it, we present a table with the results computed for a sequence of time stepping starting with $k = 0.125$ and keep on halving. "Difference" in the convergence table is obtained by $\| P_{2k} - P_k \|_\infty$, where P_k and P_{2k} are the consecutive solutions taking values $2k$ and k for the time step. "Ratio" is defined as the ratio of consecutive differences: $\frac{\|P_{4k}-P_{2k}\|_\infty}{\|P_{2k}-P_k\|_\infty}$. "Order" is computed as follows:

$$\left.\begin{array}{l} \epsilon_1 = \| P_{4k} - P_{2k} \|_\infty \\ \epsilon_2 = \| P_{2k} - P_k \|_\infty \end{array}\right\} \Rightarrow \alpha = \frac{\log \epsilon_1 - \log \epsilon_2}{\log 2}. \tag{122}$$

Table 4: Numerical convergence table for successive values of k

k	Difference	Ratio	Order
0,0125	-	-	-
0,0625	2,87874	-	-
0,03125	0,613901	4,68926	2,22936
0,015625	0,108354	5,66572	2,50226
0.0078125	0,0196251	5,52117	2,46497

It is important to show what happened if k is to high and we do not respect (113). We can see it at Figure 10

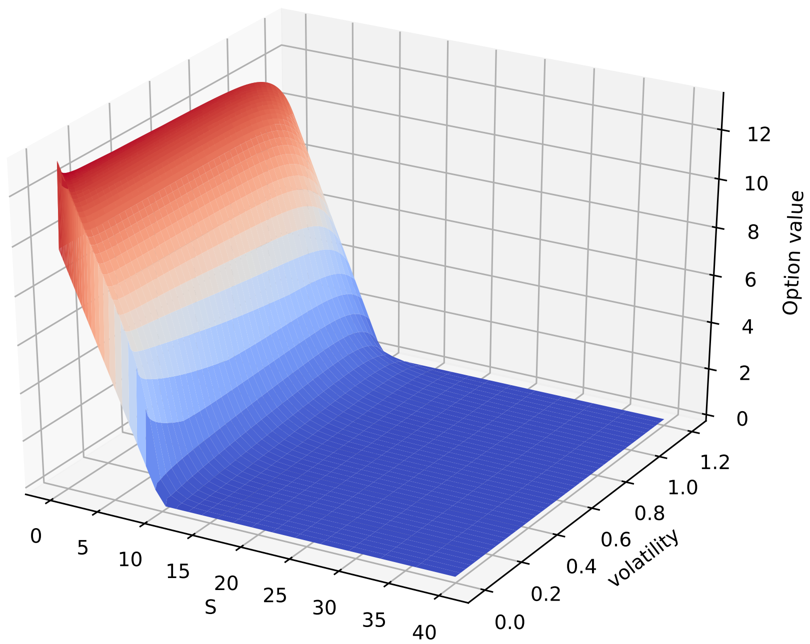

Figure 10: Numerical solutions with high k

Note that there are some asset values that surpass the strike ($E = 10$), then this solution does not satisfies the boundedness condition and implies arbitrage opportunities.

6 Conclusions

In this work we have develop a numerical method to solve American options pricing problems under stochastic volatility, we solve the non-positivity problem of cross-derivatives with the transformation (40). With the semi-discretization approach and the ETD method and we achieve a numerical scheme, whose positivity and stability is guaranteed with (96) and (113). Comparing the results with other authors we can say that we have develop a competitive and efficient method, but we also test our method and provide solutions for the case where $|\rho|$ is high, that is a case where any reference of the last thirty years have prove his competitiveness.

In future studies, it can be interesting implement extensions to the Heston model. Integrating the Bates model, which allow jumps to asset returns. Or the so-called SVCJ model, which allows jumps both asset returns and volatility.

Table 5: Models for future works

Model	Asset model	Volatility model
Heston	$dS = \mu S dt + \sqrt{\nu} S dW_1$	$d\nu = \kappa(\theta - \nu)dt + \sigma\sqrt{\nu} dW_2$
Bates	$dS = \mu S dt + \sqrt{\nu} S dW_1 + dJ$	$d\nu = \kappa(\theta - \nu)dt + \sigma\sqrt{\nu} dW_2$
SVCJ	$dS = \mu S dt + \sqrt{\nu} S dW_1 + dJ_1$	$d\nu = \kappa(\theta - \nu)dt + \sigma\sqrt{\nu} dW_2 + dJ_2$

Bibliography

Atkinson, K. (January 1989). *An Introduction to Numerical Analysis, 2nd Edition.* John Wiley & Sons.

Black, F. and Scholes, M. (1973). The pricing of options and corporate liabilities. *Journal of Political Economy*, 81(3):637–654.

Brennan, M. J. and Schwartz, E. S. (1978). Finite difference methods and jump processes arising in the pricing of contingent claims: A synthesis. *The Journal of Financial and Quantitative Analysis*, 13(3):461.

C.A. Desoer, M. (1975). *Feedback Systems: Input–Output Properties.* Academic Press.

Calvo, M., de Frutos, J., and Novo, J. (2001). Linearly implicit runge–kutta methods for advection–reaction–diffusion equations. *Applied Numerical Mathematics*, 37(4):535–549.

Casabán, M.-C., Company, R., Jódar, L., and Pintos, J.-R. (2011). Numerical analysis and computing of a non-arbitrage liquidity model with observable parameters for derivatives. *Computers & Mathematics with Applications*, 61(8):1951–1956.

Clarke, N. and Parrott, K. (1996). The multigrid solution of two-factor american put options. *Oxford Computing Laboratory, Research Report 96-16.*

Cokca, E. (2003). A computer program for the analysis of 1-d contaminant migration through a soil layer. *Environmental Modelling & Software*, 18(2):147–153.

Company, R., Egorova, V. N., and Jódar, L. (2018). Conditional full stability of positivity-preserving finite difference scheme for diffusion–advection-reaction models. *Journal of Computational and Applied Mathematics*, 341:157–168.

Company, R., Jódar, L., and Pintos, J.-R. (2009). Consistent stable difference schemes for nonlinear black-scholes equations modelling option pricing with transaction costs. *ESAIM: Mathematical Modelling and Numerical Analysis*, 43(6):1045–1061.

Company, R., Jódar, L., and Pintos, J.-R. (2010). Numerical analysis and computing for option pricing models in illiquid markets. *Mathematical and Computer Modelling*, 52(7-8):1066–1073.

Cox, J. C., Ingersoll, J. E., and Ross, S. A. (1985). A theory of the term structure of interest rates. *Econometrica*, 53(2):385.

Cox, S. and Matthews, P. (2002). Exponential time differencing for stiff systems. *Journal of Computational Physics*, 176(2):430–455.

Cryer, C. W. (1971). The solution of a quadratic programming problem using systematic overrelaxation. *SIAM Journal on Control*, 9(3):385–392.

Dahlquist, G. (1961). Stability and error bounds in the numerical integration of ordinary differential equations. 85 s. stockholm 1959. k. tekniska högskolans handlingar. *ZAMM - Zeitschrift für Angewandte Mathematik und Mechanik*, 41(6):267–268.

de la Hoz, F. and Vadillo, F. (2016). Numerical simulations of time-dependent partial differential equations. *Journal of Computational and Applied Mathematics*, 295:175–184.

Derman, E. and Kani, I. (1994). Riding on a smile. *Risk*, 7:32–39.

Duffy, D. J. (2006). *Finite Difference Methods in Financial Engineering: A Partial Differential Equation Approach.* John Wiley & Sons.

Dupire, B. (1994). Pricing with a smile. *Risk*, 7:18–20.

Düring, B. and Pitkin, A. (2019). High-order compact finite difference scheme for option pricing in stochastic volatility jump models. *Journal of Computational and Applied Mathematics*, 355:201–217.

Feller, W. (1951). Two singular diffusion problems. *The Annals of Mathematics*, 54(1):173.

Forsyth, P. A. and Vetzal, K. R. (2002). Quadratic convergence for valuing american options using a penalty method. *SIAM Journal on Scientific Computing*, 23(6):2095–2122.

Garabedian, P. R. (1998). *Partial Differential Equations*. Springer Berlin Heidelberg.

Gatheral, J. (2006). *The Volatility Surface: A Practitioner's Guide*.

Geske, R. and Johnson, H. E. (1984). The american put option valued analytically. *The Journal of Finance*, 39(5):1511–1524.

Heston, S. L. (1993). A closed-form solution for options with stochastic volatility with applications to bond and currency options. *Review of Financial Studies*, 6(2):327–343.

Hilber, N., Matache, A.-M., and Schwab, C. (2005). Sparse wavelet methods for option pricing under stochastic volatility. *The Journal of Computational Finance*, 8(4):1–42.

Hull, J. (2018). *Options, futures, and other derivatives*. Pearson Prentice Hall, Upper Saddle River, NJ [u.a.], 10. ed., pearson international edition.

Hull, J. and White, A. (1990). Valuing derivative securities using the explicit finite difference method. *The Journal of Financial and Quantitative Analysis*, 25(1):87.

Hundsdorfer, W. and Verwer, J. (2003). *Numerical Solution of Time-Dependent Advection-Diffusion-Reaction Equations*. Springer Berlin Heidelberg.

Ikonen, S. and Toivanen, J. (2007). Efficient numerical methods for pricing american options under stochastic volatility. *Numerical Methods for Partial Differential Equations*, 24(1):104–126.

Jaillet, P., Lamberton, D., and Lapeyre, B. (1990). Variational inequalities and the pricing of american options. *Acta Applicandae Mathematicae*, 21(3):263–289.

Kaczorek, T. (2002). *Positive 1D and 2D Systems*. Springer London.

Kangro, R. and Nicolaides, R. (2000). Far field boundary conditions for black–scholes equations. *SIAM Journal on Numerical Analysis*, 38(4):1357–1368.

Kassam, A.-K. and Trefethen, L. N. (2005). Fourth-order time-stepping for stiff PDEs. *SIAM Journal on Scientific Computing*, 26(4):1214–1233.

Kaya, A. (2015). Finite difference approximations of multidimensional unsteady convection–diffusion–reaction equations. *Journal of Computational Physics*, 285:331–349.

Kim, B. J., Ma, Y.-K., and Choe, H. J. (2013). A simple numerical method for pricing an american put option. *Journal of Applied Mathematics*, 2013:1–7.

Kovalov, P., Linetsky, V., and Marcozzi, M. (2007). Pricing multi-asset american options: A finite element method-of-lines with smooth penalty. *Journal of Scientific Computing*, 33(3):209–237.

Macías-Díaz, J. and Puri, A. (2012). An explicit positivity-preserving finite-difference scheme for the classical fisher–kolmogorov–petrovsky–piscounov equation. *Applied Mathematics and Computation*, 218(9):5829–5837.

Mandelbrot, B. (1967). The variation of some other speculative prices. *The Journal of Business*, 40(4):393–413.

McKean, H. P. (1965). A free boundary problem for the heat equation arising from a problem in mathematical economics. *Industrial Management Review*, 6:32–39.

Merton, R. C. (1976). Option pricing when underlying stock returns are discontinuous. *Journal of Financial Economics*, 3(1-2):125–144.

Nielsen, B. F., Skavhaug, O., and Tveito, A. (2002). Penalty and front-fixing methods for the numerical solution of american option problems. *The Journal of Computational Finance*, 5(4):69–97.

Oosterlee, C. (2003). On multigrid for linear complementarity problems with application to american-style options. *ETNA. Electronic Transactions on Numerical Analysis [electronic only]*, 15:165–185.

Pascucci, A. (2011). *PDE and Martingale Methods in Option Pricing*. Springer Milan.

Pazy, A. (1983). *Semigroups of Linear Operators and Applications to Partial Differential Equations*. Springer New York.

Persson, J. and von Sydow, L. (2010). Pricing american options using a space-time adaptive finite difference method. *Mathematics and Computers in Simulation*, 80(9):1922–1935.

P.Wilmott, S.Howison, and J.Dewynne (1995). *The Mathematics of Financial Derivatives*. Cambridge University Press.

Tangman, D., Gopaul, A., and Bhuruth, M. (2008). A fast high-order finite difference algorithm for pricing american options. *Journal of Computational and Applied Mathematics*, 222(1):17–29.

van Moerbeke, P. (1976). On optimal stopping and free boundary problems. *Archive for Rational Mechanics and Analysis*, 60(2):101–148.

Vellekoop, M. and Nieuwenhuis, H. (2009). A tree-based method to price american options in the heston model. *Journal of Computational Finance*, 13(1):1–21.

Wilmott, P. (2006). *Paul Wilmott On Quantitative Finance*. John Wiley & Sons.

Wong, B. and Heyde, C. C. (2006). On changes of measure in stochastic volatility models. *Journal of Applied Mathematics and Stochastic Analysis*, 2006:1–13.

Yousuf, M. and Khaliq, A. (2013). An efficient ETD method for pricing american options under stochastic volatility with nonsmooth payoffs. *Numerical Methods for Partial Differential Equations*, 29(6):1864–1880.

Zhu, S.-P. and Chen, W.-T. (2011). A predictor–corrector scheme based on the ADI method for pricing american puts with stochastic volatility. *Computers & Mathematics with Applications*, 62(1):1–26.

Zvan, R., Forsyth, P., and Vetzal, K. (1998). Penalty methods for american options with stochastic volatility. *Journal of Computational and Applied Mathematics*, 91(2):199–218.

Zvan, R., Forsyth, P., and Vetzal, K. (2003). Negative coefficients in two-factor option pricing models. *The Journal of Computational Finance*, 7(1):37–73.